Int J Adv Manuf Technol manuscript No.
(will be inserted by the editor)

Real-Time FDM Machine Condition Monitoring and Diagnosis based on Acoustic Emission and Hidden Semi-Markov Model

Haixi Wu · Zhonghua Yu · Yan Wang

Received: date / Accepted: date

Abstract Machine condition monitoring is considered as an important diagnostic and maintenance strategy to ensure product quality and reduce manufacturing cost. However, currently most additive manufacturing (AM) machines are not equipped with sensors for system monitoring. In this paper, a real-time lightweight AM machine condition monitoring approach is proposed, where acoustic emission (AE) sensor is used. In the proposed method, the original AE waveform signals are first simplified as AE hits, and then segmental and principal component analyses are applied to further reduce the data size and computational cost. From AE hits, the hidden semi-Markov model (HSMM) is applied to identify the machine states, including both normal and abnormal ones. Experimental studies on fused deposition modeling (FDM), one of the most popular AM technology, show that the typical machine failures can be identified in a real-time manner. This monitoring method can serve as a diagnostic tool for FDM machines.

Haixi Wu
The State Key Laboratory of Fluid Power Transmission and Control, College of Mechanical Engineering, Zhejiang University, Hangzhou, Zhejiang 310027, China
E-mail: wuhaixi@zju.edu.cn

Zhonghua Yu
The State Key Laboratory of Fluid Power Transmission and Control, College of Mechanical Engineering, Zhejiang University, Hangzhou, Zhejiang 310027, China
E-mail: yuzhh@zju.edu.cn

Yan Wang
Woodruff School of Mechanical Engineering, Georgia Institute of Technology, Atlanta, GA 30332, USA
E-mail: yan.wang@me.gatech.edu

Keywords Additive manufacturing · Fused deposition modeling · Condition monitoring · Acoustic emission · Hidden semi-Markov model

1 Introduction

Sensor-based monitoring of machine condition helps increase manufacturing process reliability and product quality, and reduce maintenance cost [20]. However, currently most additive manufacturing (AM) machines are not equipped with closed-loop monitoring and control systems [31]. With the absence of real-time sensing, process failures or machine breakdowns occur without notice during the fabrication process. Thus, the quality and repeatability of final products can not be guaranteed. There is an urgent need of implementing closed-loop monitoring and control of AM processes to allow industy to benefit from this new technology [37,35,18, 9].

Among several real-time sensing and non-destructive evaluation technologies, acoustic emission (AE) is considered to be suitable in the application to machine health monitoring, because AE sensor is sensitive to the dynamic changes of mechanical systems and it can obtain rich process information. The ease of setup and non-intrusive deployment of the AE monitoring system also makes it an attractive choice. In recent years, AE has been successfully employed for a broad variety of applications, including machine tool and process fault detection [19,1,21], material damage and surface burn detection [33,40], structural health monitoring [25,30], pharmaceutical crystallization process monitoring [15], and others.

In this work, AE sensing technique is applied to monitor AM machines. AE signal is the elastic wave-

form released in materials and can be detected by appropriate AE sensor. Typically, the continuous AE signals are recorded as original signal waveform data, and corresponding signal processing tools, such as wavelet analysis and empirical mode decomposition [8,41], can be applied to extract signal features directly for identifying conditions. This monitoring scheme is also widely used in other types of sensors such as force sensor and accelerometer [26,12]. The major drawback of this monitoring scheme is that it is difficult to store the original waveform data if high sampling rates are applied and the computational cost for signal processing is high [32]. The wide frequency range of AE sensor required for AM machine operation and the relative long fabrication time of AM processes also add extra burdens on the monitoring system. Thus, these conventional approaches can not take full advantage of AE on its high sensitivity in real time.

There is a strong need to develop an effective approach to handle the large amount of data from AE sensor and develop the corresponding big data analytics and data-driven diagnostic algorithms for sensing [29,42] in order to overcome the limitations of data storage and processing. The new application of AM process monitoring also calls for lightweight monitoring in order to ensure system flexibility, reduce manufacturing cost, and improve the product quality [10].

In this paper, a new AE-based AM machine monitoring approach is proposed. The original AE waveform signals are first simplified as AE hits, and then segmental and principal component analyses are applied to further reduce the data size and computational cost. In addition, the hidden semi-Markov model (HSMM) is chosen as the diagnostic algorithm for machine monitoring based on the processed AE data. The HSMM is a generalization of hidden Markov model (HMM). HSMM models the duration of states more efficiently than the original HMM, which focuses more on state transition [16]. Therefore HSMM is helpful to model signal segments and make inference for unobservable state based on observable sensor signals in the noisy environment [28,36]. The successful applications of HSMM for state identification and fault diagnosis include tool wear monitoring [13,14], early fault detection of gearbox [27], hydraulic pump health monitoring [11], fault diagnosis in chemical multiphase batch process [7], identification of sea regimes [6], and others. To the authors' knowledge, HSMM has not been used in monitoring AM processes.

Fused deposition modeling (FDM) is selected as the focused AM process in this study. FDM is one of the most widely used AM technology because of its relative maturity and cost-effectiveness. The FDM fabricating process is adding materials, mostly thermoplastic, in a layer-by-layer scheme. In general, AM machines go through more frequent state transitions than those in subtractive manufacturing during fabrication. It has been reported that the frequent start-stop sequences of FDM machines affect the product quality [2]. Abnormal states of machine condition, such as nozzle wear, clogging, material run-out, and filament breakage, may occur during the fabrication process [35,34]. For example, the filament breakage of FDM is illustrated in Figure 1. The machine monitoring methods that detect the abnormal states at their early stages can make quick adjustment possible thus reduce the waste of materials.

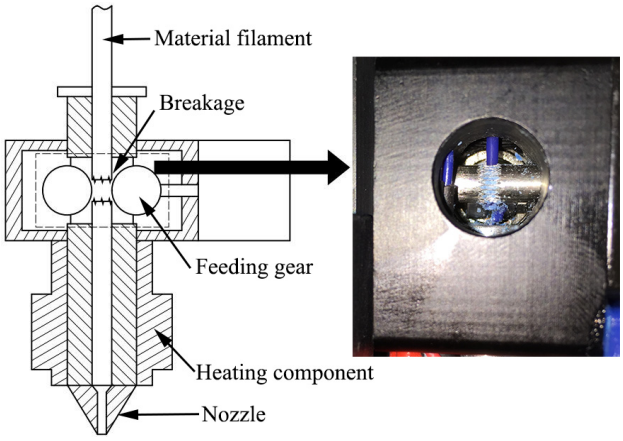

Fig. 1 A schematic drawing of material filament breakage in FDM extruder, where the image on the right shows a typical broken filament

The proposed machine monitoring method based on AE sensing and HSMM diagnostics is a further improvement and extension of our previous work [39], where support vector machine was used for classification. Here, the recorded AE signals are processed and analyzed as AE hits instead of the original waveform data in order to significantly reduced the data size. Segmental analysis and dimensionality reduction are applied to the AE hits to eliminate the hits saturation and further compress the AE data. The processed AE hits are used as inputs to train the HSMM for monitoring FDM machine conditions and the capacity of real-time diagnostics is investigated.

The rest of the paper is organized as follows. An overview of the proposed machine monitoring and diagnosis framework is provided in Section 2. The experimental setup and results are presented in Section 3, followed by a discussion in Section 4. Finally, this paper closes with a concluding remarks in Section 5.

2 Proposed Monitoring and Diagnosis Framework and Mechanisms

The framework of the proposed AE- and HSMM-based FDM machine condition monitoring and diagnosis method is shown in Figure 2. The AE waveform signals detected by the sensor are first measured as AE hits, and several features are extracted accordingly. Segmental analysis and principal component analysis (PCA) are applied on the AE hit features to reduce data size and feature vector dimension, before they become the inputs of HSMM for diagnosis. The related singal processing method and background mechanisms are described in the following subsections.

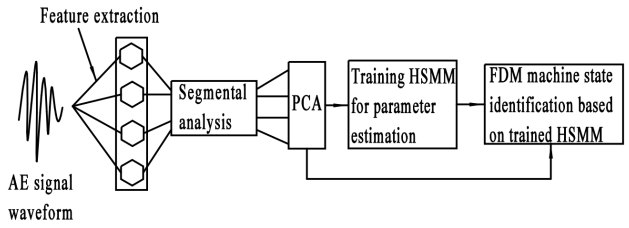

Fig. 2 The AE based framework with HSMM for FDM machine condition monitoring and diagnosis

2.1 AE signal processing and feature extraction

The AE signals collected by the sensor are measured as AE hits and then several features are extracted on the hit-level accordingly. As a result, the original massive waveform data recorded by the high-speed data acquisition (DAQ) system are parametrically compressed. Figure 3 illustrates the measurement of an AE hit and the typical features. The analyzed features in this study are amplitude, counts, duration, absolute energy (E_{abs}), signal strength (Str), and root mean square (RMS). These conventional time-domain features of AE hits are defined as follows.

Amplitude is the measured peak voltage within an AE hit. The amplitude can be expressed on a decibel (dB) scale. Counts are the total number of threshold-crossing pulses. Duration represents the elapsed time of the AE hit. Absolute energy E_{abs} is calculated as

$$E_{abs} = \alpha \int_{t_1}^{t_2} u(t)^2 dt, \tag{1}$$

where $u(t)$ is the output voltage of the AE sensor and coefficient α is inversely proportional to the AE sensor's electrical resistance. Signal strength

$$Str = \int_{t_1}^{t_2} |u(t)| dt \tag{2}$$

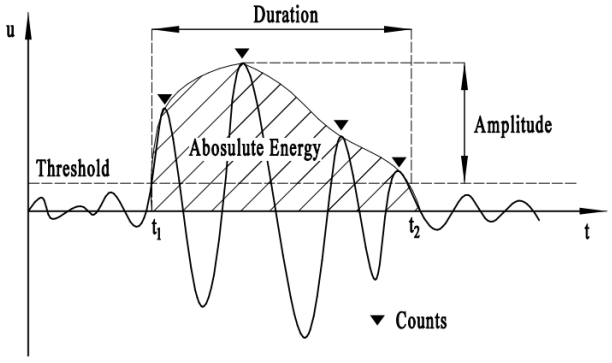

Fig. 3 Measurement of an AE hit and the typical time-domain features

is the integral of the $u(t)$ over the duration of an AE hit. RMS is defined as

$$RMS = \sqrt{\frac{1}{t_2 - t_1} \int_{t_1}^{t_2} u(t)^2 dt}. \tag{3}$$

2.2 Segmental analysis and dimensionality reduction

High-speed DAQ system can record a very large number of AE hits in real-time monitoring. In order to eliminate the hit saturation and further compress the AE data size [24], a signal segmental analysis is adopted on AE hits. The AE hits are therefore divided into short segments according to a chosen time interval, which also determines the time resolution of the monitoring method. Then the mean values of all features in each segment are calculated to represent the characteristics of the original AE signal.

After the segmental analysis and processing, the next step is to reduce the feature vector dimension based on PCA, since the multi-dimensional features of AE hits may be correlated with each other to some extent. PCA can also further alleviate the computation burdens. PCA is one of the most widely used unsupervised statistical approach for feature dimensionality reduction [22]. It finds the principal components (PCs) so that the original data can be linearly projected into this new set of coordinates with major patterns of variation represented.

Consider an AE data set $\mathbf{X} \in \mathbb{R}^{n \times p}$ with p-dimensional features extracted and a total of n data segments along time. Assume that $\mathbf{X}$ has been scaled and centered, and the column-wise mean values in the data matrix are zeros. The covariance matrix of the data set is

$$\mathbf{C} = \mathbb{E}[\mathbf{X}^T \mathbf{X}], \tag{4}$$

where $\mathbf{X}^T$ is the transpose of $\mathbf{X}$. A new k-dimensional data set $\mathbf{Y} \in \mathbb{R}^{n \times k}$ where $k \leq p$ can be derived from $\mathbf{X}$

as

$$\mathbf{Y} = \mathbf{X}\mathbf{W}, \tag{5}$$

where $\mathbf{W} \in \mathbb{R}^{p\times k}$ is the decreasing-order orthogonal basis that consists of the eigenvectors associated with the k largest eigenvalues of $\mathbf{C}$. The new data set $\mathbf{Y} = \{\mathbf{y}_1, \mathbf{y}_2, \ldots, \mathbf{y}_k\}$ is formed by the projected vectors, which are the PCs of the original AE data sample $\mathbf{X}$. Particularly, $\mathbf{y}_1$ is the direction that is associated with the maximum variance of the data, and each of the remaining components is orthogonal to the preceding ones and has the largest possible variance. The PCs are then used as the input data (observation sequence) for the HSMM training and machine state identification, described as follows.

2.3 Parameter estimation of HSMM and machine state identification

Similar to HMM, HSMM models the general time-series problems with the differentiation between observable and hidden states. A graphic model of HSMM is shown in Figure 4, where the arrow from state S_1 to state S_2 indicates the state transition, and the line connections between state sequence $\{S_t\}$ and observation sequence $\{O_t\}$ indicate the correspondences between the observations and hidden states. HSMM is modeled by parameters $\lambda = (\pi, A, D, B)$, where π is the initial probabilities, $A = \{a_{ij}\}, (i, j \in \{1, 2, \ldots, J\})$ is the transition probability matrix (TPM) for a total of J states, $D = \{d_j(u)\}$ is the state-duration distribution matrix, and the observation probability matrix is denoted by $B = \{b_j(o_t)\}$. The major difference between HSMM and HMM is the introduction of state duration D.

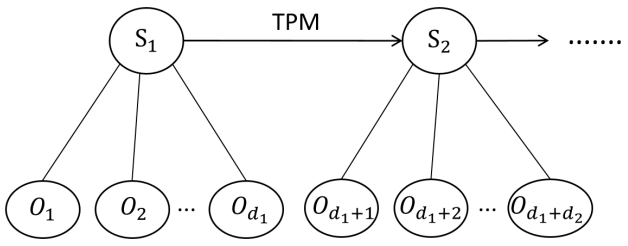

Fig. 4 The HSMM model

The initial state S_1 is determined based on the initial probabilities π_j where $j \in \{1, 2, \ldots, J\}$. Given a $\{S_t\}$ semi-Markov chain with finite state space, the first-order J-state Markov chain's initial probabilities are typically initialized as

$$\pi_j = \frac{1}{J} \tag{6}$$

with $\sum_j \pi_j = 1$. The transition probabilities

$$a_{ij} = P(S_{t+1} = j | S_{t+1} \neq i, S_t = i) \tag{7}$$

satisfy $a_{ii} = 0$ and $\sum_j a_{ij} = 1$. The duration distributions $d_j(u)$, also known as the sojourn time distribution, model the duration of the system remaining at state $S_t = j$. The semi-Markov chain $\{S_t\}$ is the combination of the first-order Markov chain and duration distribution.

The state sequence $\{S_t\}$ can be only evaluated indirectly through the observation sequence $\{O_t\}$. The discrete observation sequence $\{O_t\}$ is associated to the semi-Markov chain $\{S_t\}$ by the observation probabilities

$$b_j(o_t) = P(O_t = o_t | S_t = j). \tag{8}$$

In this study, the input data for HSMMs are the PCs processed from the original AE data set. The HSMM parameter estimation during the model training process is based on the expectation-maximization (EM) algorithm for the right-censored HSMM [16]. The basic procedure of the EM algorithm is that the model parameters are iteratively updated through the iteration of the so-called E- and M-step until the lower bounds on the log-likelihood converge and reach an error threshold or the maximum number of iterations is reached. Here, the convergence error is set to 10^{-8}, and the maximum iteration count is set to 50.

Once the training is finished, the next step is to identify the FDM machine states for diagnosis from new observation sequences based on the trained HSMM. This procedure is based on the so-called decoding process which finds the most probable hidden state sequence according to the observation sequence. The Viterbi algorithm that performs a global decoding is the most popular algorithm in solving this problem. The Viterbi algorithm computes the most probable sequence of unobservable states given the observation sequence, which finds

$$\arg \max_{j_1,\ldots,j_t} P(S_1 = j_1, \ldots, S_t = j_t | O_1^t = o_1^t). \tag{9}$$

The details of the EM and Viterbi algorithms can be found in [16,4]. The R implementation of HSMM [5] is used in this study. Specifically, the observation distribution is assumed to be a Gaussian distribution, which is derived from our training data. The duration distribution is modeled as a logarithmic distribution based on our sensor data.

3 Experimental Study

In this section, an experimental study of real-time monitoring of the FDM extruder condition based on the proposed method is described.

3.1 Experiment set up

In the experiment, an AE sensor is mounted on the Model E5 Engine FDM machine made by HYREL3D. The selected AE sensor is a wide-band differential sensor with a wide response range of $100 - 900$ kHz. The differential sensor allows the background noise to be reduced by approximately 2 dB. The AE sensor is attached to the FDM machine's extruder with vacuum grease. The installation of the AE sensor is shown in Figure 5. PAC 2/4/6 and PAC PCI-2, both made by Mistras Group, are used as the preamplifier and DAQ system respectively. The selected gain of the preamplifier is 40 dB, and the threshold value of the DAQ system is 58 dB. The A/D conversion scheme of this DAQ system is 18-bit, and the sampling rate in this study is set to be $5M$ samples per second in order to maintain the information integrity and AE data flow rate.

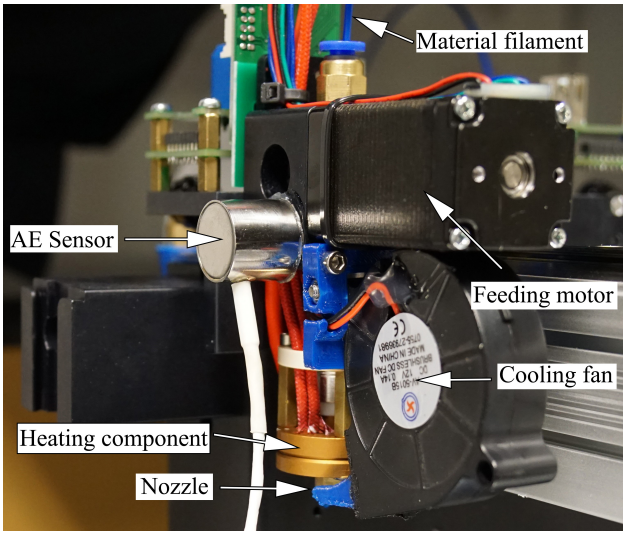

Fig. 5 Installation of AE sensor

3.2 Experimental procedure

Several machine operating conditions including both normal and abnormal states are intentionally generated in the experiment, while AE signals are continuously collected by the AE system. The controlled operation sequence of the FDM machine is shown in Figure 6, where material filament is loaded, extruded, and unloaded within a period of time. Four machine states are assumed, which are extruding without material as State 1, material loading/unloading as State 2, idle as State 3, and normal extruding as State 4. These four represent the major states of the machine conditions. The state of extruding without material is the typical abnormal state when material runs out or there is filament breakage [34,39]. These two failure modes occur when material filament cannot be fed in by the feeding motor and gear.

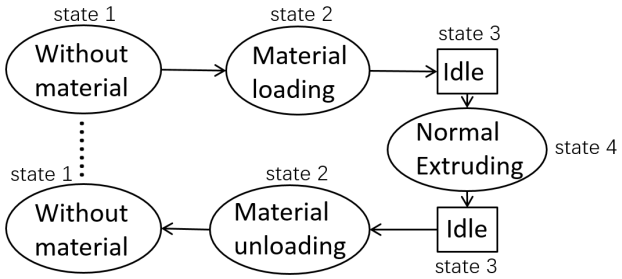

Fig. 6 Operation sequence of FDM extruder in the experiment

Based on the methods described in Section 2, the recorded AE signals are processed with features identified by the advanced DAQ system. The PCs of features are extracted. After the HSMM is trained, new observation sequences are taken to test the diagnosis function. Our previous study [39] shows that the time-domain features of AE hits are closely related to the machine operating conditions and state transitions. Thus features in the time domain are the focus of this work.

3.3 Experimental results and AE data analysis

The segmental analysis was applied to the extracted AE features first. The chosen time interval or the time resolution of the monitoring method was $0.1s$. A total number of 581 segments were divided from the experimental process of $58.1s$. The total number of the record AE hits was $29,523$. Thus approximately 51 AE hits were located in each segment. After segmental analysis, the data size is significantly reduced.

The mean values of six time-domain features for each segment from the AE hits, which were simultaneously recorded in the experiment, are displayed in Figure 7(a)-(f). It is seen that machine state transitions can be detected with the trend of feature value changes. Though the mean values of these features may still vary with different measurement scales, the influence of random fluctuation and measurement noise can be

eliminated with the averaging procedure. It is observed that the state of extruding without material (State 1), roughly before segment No. 100 and after segment No. 450, has the highest mean values of all six AE features, which suggests that the abnormal FDM machine conditions of material run-out or filament breakage are largely reflected and sensitive enough for the changes of these time-domain AE hits. It is also noted that the characteristics of the feature distributions of the material loading and unloading state (State 2), approximately between segment No. 100 and No. 200, versus between segment No. 350 and No. 450, are similar. This is because the only difference between these two states is the feeding gear and motor are running at opposite directions and their dynamic characteristics resemble.

One can also tell from Figure 7 that these six time-domain AE features are correlated to certain extent, as they show a similar trend during the FDM machine state transitions. However, the sensitivities of these features vary during different state transitions. For instance, the Amplitude feature has significant value shifts to and from the idle state (approximately between segment No. 200 and 230, between No. 320 and No. 350). but the difference between the material loading/unloading (State 2) and normal extruding (State 4, approximately between No. 230 and No. 320) for Amplitude are not obvious. In contrast, the AE features of counts and duration show distinct changes between the material loading/unloading and normal extruding states, whereas their differences between loading/unloading and idle are not obvious. The changes of RMS are not distinct between State 2 and State 4. The sensitivity variation among features with respect to different states indicates that no single AE feature is representative enough for state identification if these features in original signals are to be used.

For the purpose of reducing feature dimensionality while ensuring the major variance captured, the PCA is used to project the six features of original AE hits to a lower-dimensional space. The variance ranking of PCs as the result of PCA is shown in Figure 8 (a). It can be seen that the first principal component PC1 captures most of the variance, which is 91.2% of the total variance. The values of all six calculated principal components (PC1 - PC6) are displayed in Figure 8 (b). From the PCs, states and state transition can be identified more easily than the original AE features.

According to the Kaiser criterion [23], the principal components with the variance greater than 1.00 are retained. Therefore, the first principal component (PC1) was selected for the following study of HSMM-based training and machine state identification. PC1 represents the main characteristics of the original AE data, as the four different FDM machine states and transitions can be observed directly. As a result, the previous issue of sensitivity variation in original AE features with respect to different states is resolved. There is no need to use all six dimensions of features, which significantly reduces computational cost associated with HSMM.

3.4 HSMM training and FDM machine state identification

The first principal component PC1 from PCA is used for HSMM parameter estimation. The training data set contains 80% of the total segments in PC1, and the rest 20% is used to test the accuracy of state identification. Thus, the numbers of segments for training and testing were 464 and 117 respectively.

During the training, the initial values of the initial probabilities are set to be $\pi_0 = [1/4, 1/4, 1/4, 1/4]$. The initial values for the TPM is

$$A_0 = \begin{bmatrix} 0, & 1/3, & 1/3, & 1/3 \\ 1/3, & 0, & 1/3, & 1/3 \\ 1/3, & 1/3, & 0, & 1/3 \\ 1/3, & 1/3, & 1/3, & 0 \end{bmatrix}.$$

The initial parameters for the state-duration distribution, which is given by a logarithmic distribution, are

$$p_0 = [0.9800, 0.9800, 0.9800, 0.9800].$$

The observation probabilities are given as Gaussian distributions with means

$$\mu_0 = [2.5504, -1.9940, -3.2017, -0.3652]$$

and variances

$$\sigma_0^2 = [0.8144, 0.5738, 0.8164, 0.8110],$$

which are estimated from the PC1 in different states.

The parameter estimation process was performed based on the EM algorithm mentioned in Section 2.3. The log-likelihood increases monotonically during the iterative training process, as shown in Figure 9. The log-likelihood reaches the preset threshold at iteration 21. This training process indicates that the HSMM has the capability of rapid learning, which is important for real-time performance. The final estimated values of the initial probabilities is $\pi = [1, 0, 0, 0]$, and the estimated values for the TPM is

$$A = \begin{bmatrix} 0, & 0.3940, & 0.3041, & 0.3018 \\ 0.5785, & 0, & 0.1169, & 0.3045 \\ 0.3658, & 0.4809, & 0, & 0.1531 \\ 0.6097, & 0.1540, & 0.2361, & 0 \end{bmatrix}.$$

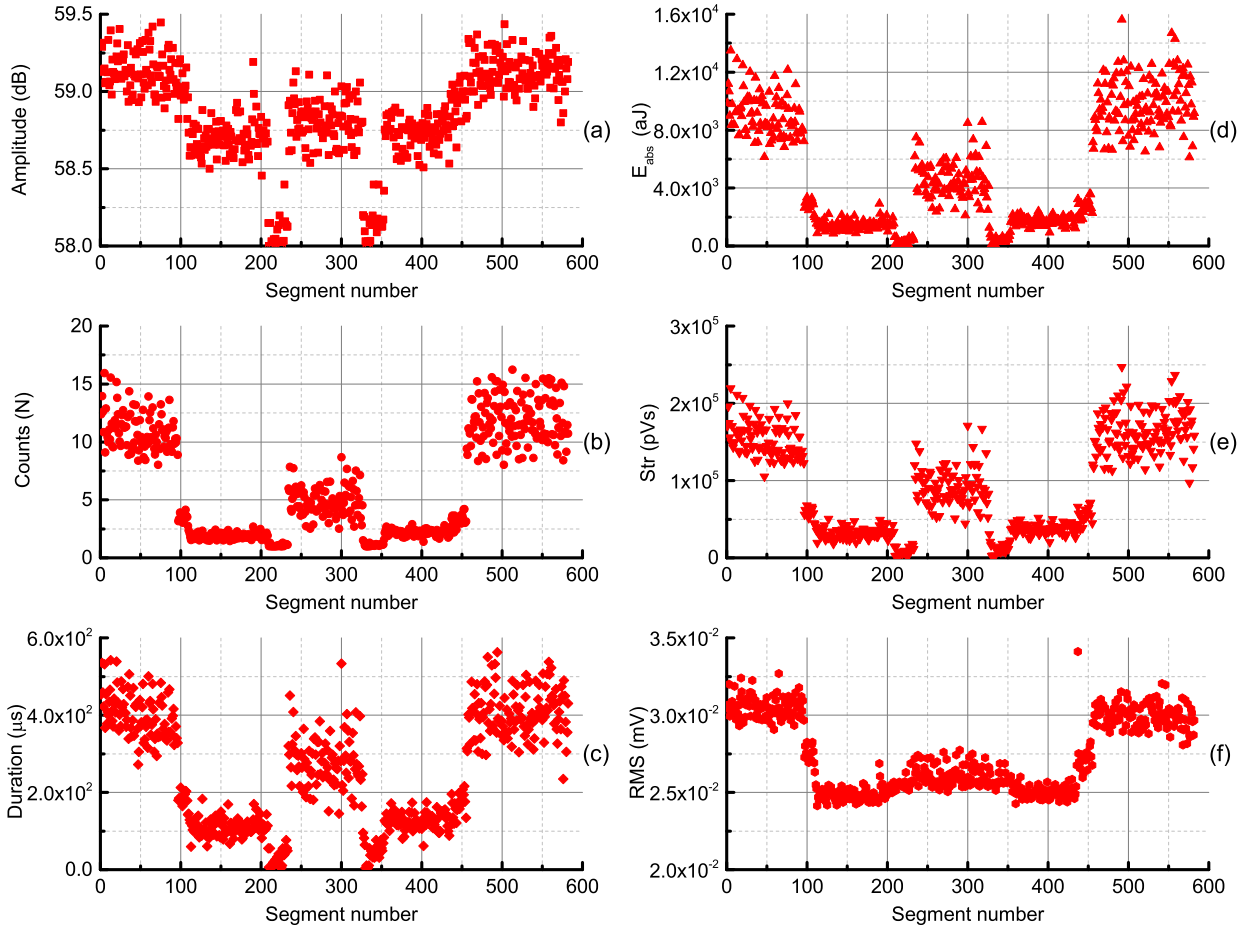

Fig. 7 Mean values of the six time-domain features for AE hit segments

The estimated parameters of logarithmic distributions for the state-duration probabilities are

$$p = [0.5974, 0.4243, 0.3419, 0.3277].$$

The estimated means and variances for the observation probability matrix are

$$\mu = [2.6102, -2.0456, -2.6945, -0.4783]$$

and

$$\sigma^2 = [0.7685, 0.1241, 0.4249, 0.2835].$$

By applying the Viterbi algorithm, the most probable FDM machine states can be obtained from the test data set. The identification results of the 117 test segments are presented in Figure 10. The state sequences of the input PC1 data were inferred by the trained HSMM. The identification accuracy of the HSMM is 93.2%, where 109 segments from test data are recognized correctly and only 8 segments are mis-identified.

To further evaluate the diagnosis accuracy, the trained HSMM was further applied to identify the state transitions during the entire experimental process, and the identification results are presented in Figure 11. The overall identification accuracy is 91.9%, where 534 out of the total 581 segments based on PC1 are identified correctly. The statistics of the identification results are provided in Table 1. The relative high unweighted kappa values indicate a good agreement of these cross-validation analysis [38].

3.5 Sensitivity analysis of the identification

The sensitivity of the identification accuracy is analyzed with two other time resolutions. The same procedures as described in Section 2 for AE data processing and HSMM training were followed, with the only differences of the chosen segment lengths.

The state identification result under the time resolution of $0.05s$ and $0.2s$ are shown in Figure 12(a) and (b) respectively. In the first sensitivity analysis with the

Table 1 Statistical analysis of identification results

	Test data	All data
Total segment number	117	581
Correctly identified segments	109	534
Accuracy rate	93.2%	91.9%
95% confidence interval	(0.8697, 0.97)	(0.8939, 0.94)
Kappa	0.9012	0.8832

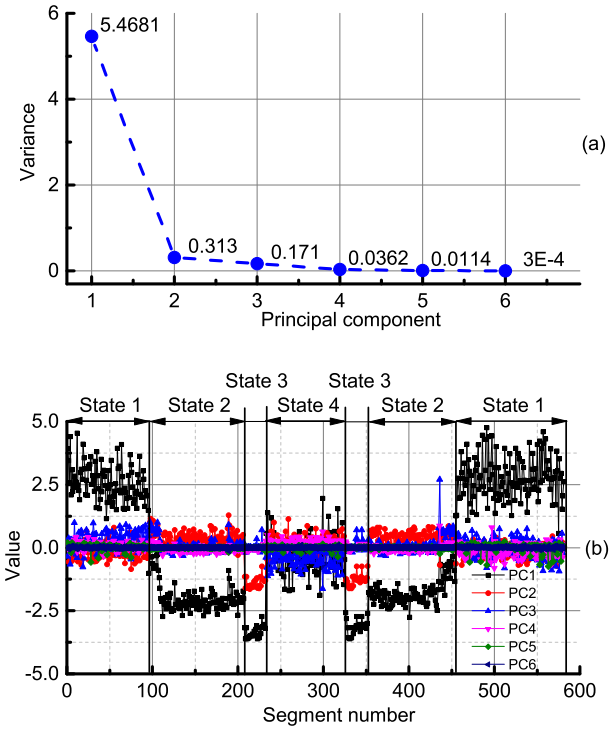

Fig. 8 Results of the PCA including (a) the scree plot of PCA and (b) values of all 6 PCs

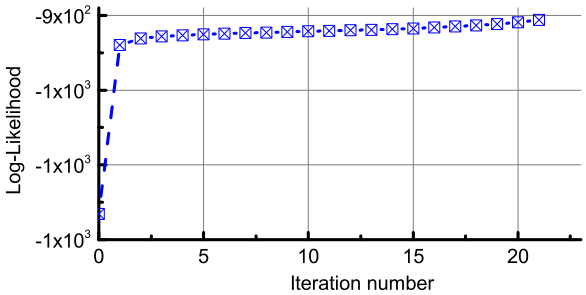

Fig. 9 The training curve of the HSMM

time resolution of 0.05s, a total number of 1162 segments were generated, of which 20%, or 233 segments, were randomly selected as the test data set. The identification accuracy of this data set is 86.27%, and the number of iterations to train HSMM is 27. In the second sensitivity study, the time resolution of 0.2s is chosen,

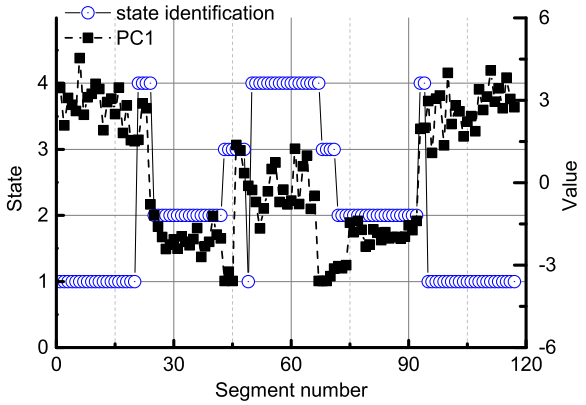

Fig. 10 The results of FDM machine state identification for the test data segments of PC1

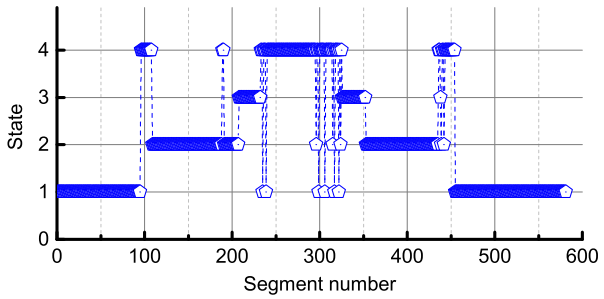

Fig. 11 The results of FDM machine state identification for all data segments of PC1

and the total number of segments is 290. 56 out of the 58 test segments were identified correctly. The identification accuracy is 96.55%. The HSMM converges with only 8 iterations during the training process in this case. However, the reduced time resolution may affect the response for real-time monitoring.

Sensitivity analysis shows that, although the majority of the FDM machine states can be identified by the proposed monitoring method, the selection of the time resolution and segment length can affect the overall performance. Therefore, the selection of 0.1s as the time interval could maintain a proper balance between identification accuracy and computational cost under this monitoring scheme for FDM machine.

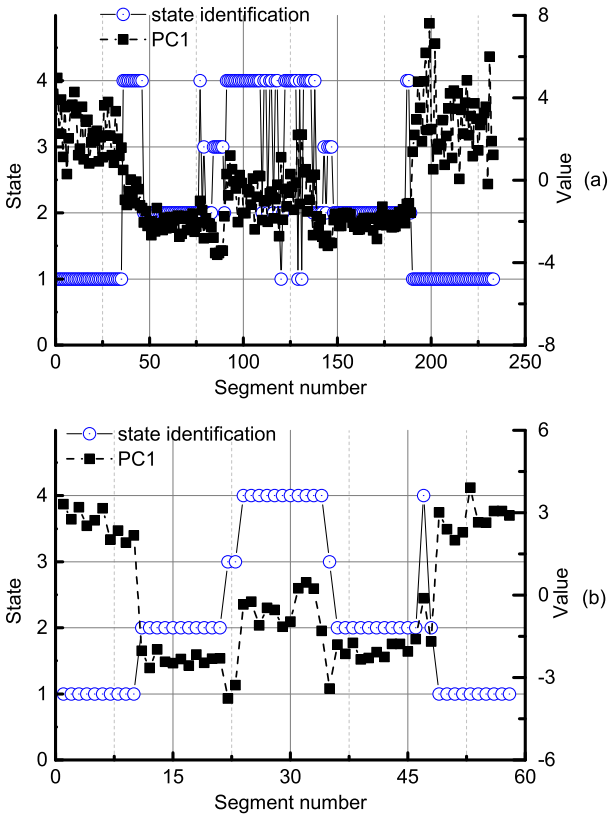

Fig. 12 FDM machine state identification results with different time resolutions of (a) $0.05s$ and (b) $0.2s$

4 Discussions

From the experimental results and analyses, it is seen that the proposed AE- and HSMM-based FDM machine monitoring and diagnosis method can identify the major operating conditions of the extruder. The typical abnormal states of material run-out or filament breakage can be detected in a real time manner with efficient training and learning.

There are mainly two performance improvements of the method proposed in this paper compared to our previous support vector machine (SVM) based method [39]. The first one is that the dimensions of time-domain AE features are systematically reduced by using PCA. Thus the robustness and generality of the monitoring method are improved. With the reduced dimensionality and sizes of input AE data, lightweight and efficient machine learning is good for real-time applications. A reasonable accuracy (greater than 90%) can be achieved under the time resolution of $0.1s$. Second, HSMM has the advantage of multi-state identification compared to SVM, which is basically for binary classification. To identify a total of k states, $k(k-1)/2$ trained SVM models may be needed based on the one-against-one strategy, and k SVM models are needed if the one-against-all strategy is used [17]. In contrast, in HSMM, the most probable state can be obtained directly via Viterbi algorithm. HSMM is a more versatile model for the application of machine condition diagnosis with the consideration of sensing errors because it introduces the relation between observable and hidden states. Furthermore, the prediction of state transitions in HSMM also provides an integrated prognosis approach.

A small number of segments were mis-identified by HSMM, which is mostly because of the overlaps of the original data as observed in Figure 8 (c), such as among segment No. 96-110, No. 435-455 and State 4. These two obvious AE spikes were seen particularly at the beginning of the material loading state and at the end of the material unloading state. This phenomenon is very similar to the entry and exit AE spikes that were detected on the grinding process [3]. The cause of these overlaps could be the sudden changes of machine dynamics, electrical current fluctuations, and instability of the extruding process. Consequently, methods for noise removal or suppression on the AE hits need further investigation in future study for more accurate state identification.

5 Concluding Remarks

In this paper, a real-time and lightweight FDM machine condition monitoring and diagnosis method is presented. Its application to identify operation conditions of the FDM machine's extruder, including both normal and abnormal states, is demonstrated. Experiments were carried out to identify four typical FDM extruder states and transitions. AE signals from the experiments were recorded by a high-speed data acquisition system. Six time-domain features of the recorded AE hits were analyzed and principal components were extracted. The size of AE data was significantly reduced while the important information and the characteristics for diagnosis were kept. Consequently, the complexity of the computation for machine learning was also reduced. One principal component was used for HSMM parameter estimation and state identification. The experimental results show that the proposed method can detect common machine failures such as material run-out or filament breakage. This method could be applied as a real-time diagnostic tool for FDM machine condition monitoring to improve printing process reliability and product quality.

Acknowledgements Wu and Yu were supported in part by the National Natural Science Foundation of China (Grant No. 51675481). Wu was also supported by China Scholarship Council with a scholarship (No. 201406320108) and is thank-

ful to Dr. Jian Qiu for discussions. The authors appreciate the comments from anonymous reviewers.

References

1. Al-Ghamd, A.M., Mba, D.: A comparative experimental study on the use of acoustic emission and vibration analysis for bearing defect identification and estimation of defect size. Mechanical Systems and Signal Processing **20**(7), 15371571 (2006). DOI 10.1016/j.ymssp.2004.10.013
2. Armillotta, A.: Assessment of surface quality on textured fdm prototypesnull. Rapid Prototyping Journal **12**(1), 3541 (2006). DOI 10.1108/13552540610637255
3. Babel, R., Koshy, P., Weiss, M.: Acoustic emission spikes at workpiece edges in grinding: Origin and applications. International Journal of Machine Tools and Manufacture **64**, 96101 (2013). DOI 10.1016/j.ijmachtools.2012.08.004
4. Bulla, J., Bulla, I.: Stylized facts of financial time series and hidden semi-markov models. Computational Statistics & Data Analysis **51**(4), 21922209 (2006). DOI 10.1016/j.csda.2006.07.021
5. Bulla, J., Bulla, I., Nenadi, O.: hsmm an r package for analyzing hidden semi-markov models. Computational Statistics & Data Analysis **54**(3), 611619 (2010). DOI 10.1016/j.csda.2008.08.025
6. Bulla, J., Lagona, F., Maruotti, A., Picone, M.: A multivariate hidden markov model for the identification of sea regimes from incomplete skewed and circular time series. Journal of Agricultural, Biological, and Environmental Statistics **17**(4), 544567 (2012). DOI 10.1007/s13253-012-0110-1
7. Chen, J., Jiang, Y.C.: Development of hidden semi-markov models for diagnosis of multiphase batch operation. Chemical Engineering Science **66**(6), 10871099 (2011). DOI 10.1016/j.ces.2010.12.009
8. Chen, X., Li, B.: Acoustic emission method for tool condition monitoring based on wavelet analysis. The International Journal of Advanced Manufacturing Technology **33**(9-10), 968976 (2006). DOI 10.1007/s00170-006-0523-5
9. US Department of Commerce, N.: Roadmapping workshop: Measurement science for prognostics and health management of smart manufacturing systems. URL http://www.nist.gov/el/isd/phm4sms-workshop.cfm
10. Conner, B.P., Manogharan, G.P., Martof, A.N., Rodomsky, L.M., Rodomsky, C.M., Jordan, D.C., Limperos, J.W.: Making sense of 3-d printing: Creating a map of additive manufacturing products and services. Additive Manufacturing **14**, 6476 (2014). DOI 10.1016/j.addma.2014.08.005
11. Dong, M., He, D.: A segmental hidden semi-markov model (hsmm)-based diagnostics and prognostics framework and methodology. Mechanical Systems and Signal Processing **21**(5), 22482266 (2007). DOI 10.1016/j.ymssp.2006.10.001
12. Feng, Z., Liang, M., Chu, F.: Recent advances in timefrequency analysis methods for machinery fault diagnosis: A review with application examples. Mechanical Systems and Signal Processing **38**(1), 165205 (2013). DOI 10.1016/j.ymssp.2013.01.017
13. Geramifard, O., Xu, J.X., Zhou, J.H., Li, X.: Continuous health condition monitoring: A single Hidden Semi-Markov Model approach, p. 110 (2011). DOI 10.1109/ICPHM.2011.6024333
14. Geramifard, O., Xu, J.X., Zhou, J.H., Li, X.: A physically segmented hidden markov model approach for continuous tool condition monitoring: Diagnostics and prognostics. IEEE Transactions on Industrial Informatics **8**(4), 964973 (2012). DOI 10.1109/TII.2012.2205583
15. Gherras, N., Serris, E., Fevotte, G.: Monitoring industrial pharmaceutical crystallization processes using acoustic emission in pure and impure media. International Journal of Pharmaceutics **439**(12), 109119 (2012). DOI 10.1016/j.ijpharm.2012.09.048. 00009
16. Gudon, Y.: Estimating hidden semi-markov chains from discrete sequences. Journal of Computational and Graphical Statistics **12**(3), 604639 (2003). DOI 10.1198/1061860032030
17. Hsu, C.W., Lin, C.J.: A comparison of methods for multiclass support vector machines. IEEE Transactions on Neural Networks **13**(2), 415425 (2002). DOI 10.1109/72.991427. 05208
18. Huang, Y., Leu, M.C., Mazumder, J., Donmez, A.: Additive manufacturing: Current state, future potential, gaps and needs, and recommendations. Journal of Manufacturing Science and Engineering **137**(1), 014,001014,001 (2015). DOI 10.1115/1.4028725
19. Hung, C.W., Lu, M.C.: Model development for tool wear effect on ae signal generation in micromilling. The International Journal of Advanced Manufacturing Technology **66**(9-12), 18451858 (2013). DOI 10.1007/s00170-012-4464-x
20. Jardine, A.K.S., Lin, D., Banjevic, D.: A review on machinery diagnostics and prognostics implementing condition-based maintenance. Mechanical Systems and Signal Processing **20**(7), 14831510 (2006). DOI 10.1016/j.ymssp.2005.09.012
21. Jian, H., Lee, H.R., Ahn, J.H.: Detection of bearing/rail defects for linear motion stage using acoustic emission. International Journal of Precision Engineering and Manufacturing **14**(11), 20432046 (2013). DOI 10.1007/s12541-013-0256-y
22. Jolliffe, I.: Principal component analysis. Wiley Online Library (2002)
23. Kaiser, H.F.: The application of electronic computers to factor analysis. Educational and psychological measurement (1960)
24. Kharrat, M., Ramasso, E., Placet, V., Boubakar, M.L.: A signal processing approach for enhanced acoustic emission data analysis in high activity systems: Application to organic matrix composites. Mechanical Systems and Signal Processing **7071**, 10381055 (2016). DOI 10.1016/j.ymssp.2015.08.028
25. Kral, Z., Horn, W., Steck, J.: Crack propagation analysis using acoustic emission sensors for structural health monitoring systems. The Scientific World Journal **2013** (2013). DOI 10.1155/2013/823603. URL http://www.hindawi.com/journals/tswj/2013/823603/abs/
26. Lei, Y., Lin, J., He, Z., Zuo, M.J.: A review on empirical mode decomposition in fault diagnosis of rotating machinery. Mechanical Systems and Signal Processing **35**(12), 108126 (2013). DOI 10.1016/j.ymssp.2012.09.015
27. Lin, C.: Early fault detection and optimal maintenance control for partially observable systems subject to vibration monitoring. Ph.D. thesis (2014). URL https://tspace.library.utoronto.ca/handle/1807/68266
28. Liu, Q., Dong, M., Lv, W., Geng, X., Li, Y.: A novel method using adaptive hidden semi-markov model for multi-sensor monitoring equipment health prognosis. Mechanical Systems and Signal Processing **6465**, 217232 (2015). DOI 10.1016/j.ymssp.2015.03.029

29. Manyika, J., Chui, M., Brown, B., Bughin, J., Dobbs, R., Roxburgh, C., Byers, A.H.: Big data: The next frontier for innovation, competition, and productivity (2011)
30. Niri, E.D., Farhidzadeh, A., Salamone, S.: Adaptive multisensor data fusion for acoustic emission source localization in noisy environment. Structural Health Monitoring **12**(1), 5977 (2013). DOI 10.1177/1475921712462937
31. Pei, E., Campbell, R.I., de Beer, D.: Entry-level rp machines: how well can they cope with geometric complexity? Assembly Automation **31**(2), 153160 (2011). DOI 10.1108/01445151111117737
32. Peng, Z.K., Chu, F.L.: Application of the wavelet transform in machine condition monitoring and fault diagnostics: a review with bibliography. Mechanical Systems and Signal Processing **18**(2), 199221 (2004). DOI 10.1016/S0888-3270(03)00075-X
33. Ramasso, E., Placet, V., Boubakar, M.: Unsupervised consensus clustering of acoustic emission time-series for robust damage sequence estimation in composites. IEEE Transactions on Instrumentation and Measurement **64**(12), 32973307 (2015). DOI 10.1109/TIM.2015.2450354
34. Rao, P., Liu, J., Roberson, D., Kong, Z.J., Williams, C.: Online real-time quality monitoring in additive manufacturing processes using heterogeneous sensors. Journal of Manufacturing Science and Engineering **137**(6), 61,007 (2015). DOI 10.1115/1.4029823
35. Reutzel, E.W., Nassar, A.R.: A survey of sensing and control systems for machine and process monitoring of directed-energy, metal-based additive manufacturing. Rapid Prototyping Journal **21**(2), 159167 (2015). DOI 10.1108/RPJ-12-2014-0177
36. Springer, D.B., Tarassenko, L., Clifford, G.D.: Logistic regression-hsmm-based heart sound segmentation. IEEE Transactions on Biomedical Engineering **63**(4), 822832 (2016). DOI 10.1109/TBME.2015.2475278
37. Tapia, G., Elwany, A.: A review on process monitoring and control in metal-based additive manufacturing. Journal of Manufacturing Science and Engineering **136**(6), 060,801060,801 (2014). DOI 10.1115/1.4028540
38. Viera, A.J., Garrett, J.M., et al.: Understanding interobserver agreement: the kappa statistic. Fam Med **37**(5), 360–363 (2005)
39. Wu, H., Wang, Y., Yu, Z.: In situ monitoring of fdm machine condition via acoustic emission. The International Journal of Advanced Manufacturing Technology p. 113 (2015). DOI 10.1007/s00170-015-7809-4
40. Yang, Z., Yu, Z., Wu, H., Chang, D.: Laser-induced thermal damage detection in metallic materials via acoustic emission and ensemble empirical mode decomposition. Journal of Materials Processing Technology **214**(8), 16171626 (2014). DOI 10.1016/j.jmatprotec.2014.03.009
41. Yang, Z., Yu, Z., Xie, C., Huang, Y.: Application of hilberthuang transform to acoustic emission signal for burn feature extraction in surface grinding process. Measurement **47**, 1421 (2014). DOI 10.1016/j.measurement.2013.08.036
42. Zaslavsky, A., Perera, C., Georgakopoulos, D.: Sensing as a service and big data. arXiv:1301.0159 [cs] (2013). URL http://arxiv.org/abs/1301.0159. ArXiv: 1301.0159